Time-Resolved Measurements of the Photolysis and Recombination of Adenosylcobalamin Bound to Glutamate Mutase

Roseanne J. Sension,* D. Ahmasi Harris, Andrew Stickrath, Allwyn G. Cole, Christel C. Fox, and E. Neil G. Marsh*

Departments of Chemistry and of Physics, University of Michigan, Ann Arbor, Michigan 48109-1055

Received: May 12, 2005; In Final Form: July 15, 2005

Femtosecond to nanosecond transient absorption spectroscopy is used to investigate the photolysis of 5′-deoxyadenosylcobalamin (coenzyme B_{12}, AdoCbl) bound to glutamate mutase. The photochemistry of AdoCbl is found to be inherently dependent upon the environment of the cofactor. Excitation of AdoCbl bound to glutamate mutase results in formation of a metal-to-ligand charge transfer intermediate state which decays to form cob(II)alamin with a time constant of 105 ps. This observation is in contrast to earlier measurements in water where the photohomolysis proceeds through an intermediate state in which the axial dimethylbenzimidazole ligand appears to have dissociated, and measurements in ethylene glycol where prompt bond homolysis is observed (Yoder, L. M.; Cole, A. G.; Walker, L. A., II; Sension, R. J. *J. Phys. Chem. B* **2001**, *105*, 12180−12188). The quantum yield for formation of stable radical pairs in the enzyme is found to be $\phi = 0.05 \pm 0.03$, and the resulting intrinsic rate constants for geminate recombination and "cage escape" are 1.0 ± 0.1 and 0.05 ± 0.03 ns^{-1}, respectively. The rate constant for geminate recombination is 30% less than that observed for AdoCbl in water or ethylene glycol. This reduction is insufficient to account for the 10^{12}-fold increase in the homolysis rate observed when substrate is bound to the protein. Finally, the protein provides a cage to prevent diffusive loss of the adenosyl radical; however, the ultimate yield for long-lived radicals is determined by the evolution from a singlet to a triplet radical pair as proposed for AdoCbl in ethylene glycol.

I. Introduction

Adenosylcobalamin (coenzyme B_{12}, AdoCbl) dependent enzymes catalyze a variety of chemically unusual rearrangement reactions that proceed via mechanisms involving organic radicals.[1−3] These radicals are initially generated by homolysis of the coenzyme cobalt−carbon bond to produce 5′-deoxyadenosyl radical and cob(II)alamin (Cbl(II)) (Figure 1). An important and poorly understood aspect of the mechanism is how the protein modulates the reactivity of the coenzyme to weaken the carbon−cobalt bond and facilitate homolytic bond cleavage. In free solution at room temperature, the bond dissociation energy of the Co−C bond is 32 kcal/mol and the half-time for homolysis is estimated to be about 6 months.[4−6] On the other hand, when AdoCbl is bound to an enzyme, homolysis occurs within milliseconds in response to substrate binding. The overall result is a $\sim 10^{12}$-fold acceleration in the rate of AdoCbl homolysis.[7]

Several different hypotheses have been advanced to explain how the enzyme may accelerate homolysis of AdoCbl. One of the most often discussed has dealt with the potential influence of the trans-axial nitrogenous ligand on the strength of the Co−C bond. In one class of AdoCbl-dependent isomerases, typified by diol dehydratase,[8] the axial dimethylbenzimidazole (DMB) ligand remains coordinated to the cobalt when bound to the protein. However, in another class of AdoCbl-dependent enzymes, typified by glutamate mutase[9] and methylmalonyl-CoA mutase,[10] a histidine residue of the protein supplies the axial ligand (see Figure 2). The potential influence of the protein on this trans-axial ligand has been one focus of a number of studies seeking to understand the mechanism for control of the Co−C bond.

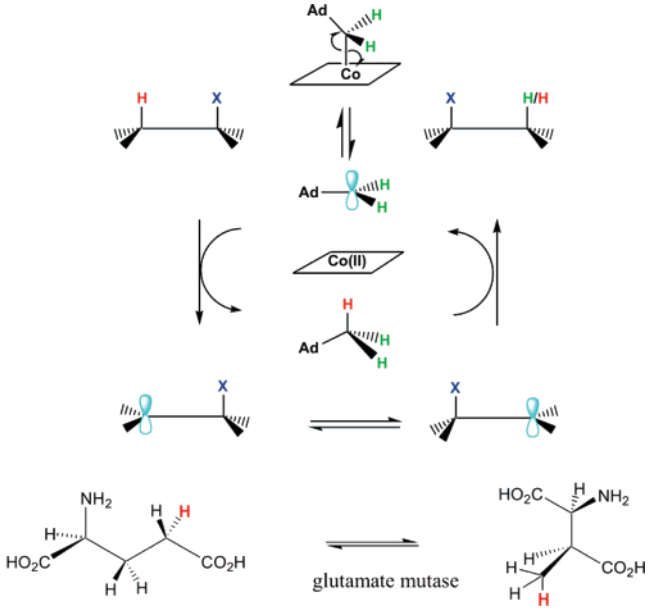

Figure 1. Top: General scheme for the radical hydrogen 1,2-migration reactions catalyzed by AdoCbl-dependent isomerases. The migrating hydrogen is shown in red. Hydrogens from the coenzyme that may exchange with the substrate are shown in green. The migrating group, X, may be HO−, NH_2−, or a carbon-containing fragment, as in the case of glutamate mutase. Bottom: Reaction catalyzed by glutamate mutase, with the position of the migrating hydrogen shown in red.

* To whom correspondence should be addressed. E-mail: rsension@umich.edu (R.J.S.); nmarsh@umich.edu (E.N.G.M.).

10.1021/jp052492d CCC: $30.25
Published on Web 09/02/2005

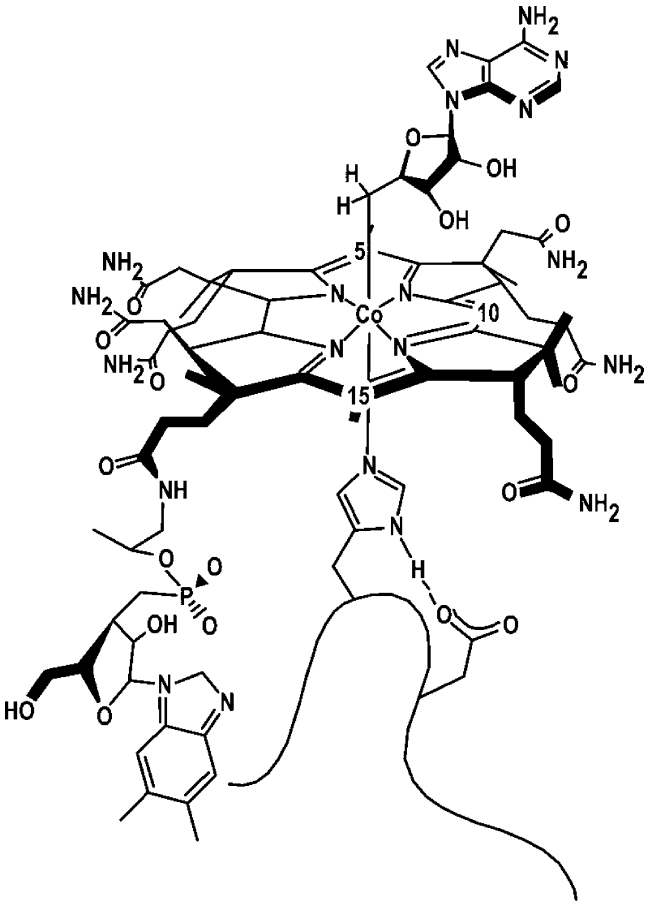

Figure 2. Schematic diagram of adenosylcobalamin as bound to glutamate mutase. The His 14 residue of the MutS protein provides the lower axial ligand to the cobalt. This residue is connected via a hydrogen bond to the Asp 14 on MutS. The plane of the corrin ring has carbons numbered 5, 10, and 15 indicated. A line between C5 and C15 defines the long axis of the corrin ring, while a line containing the Co and C-10 defines the short axis. The principle electronic transition of the cobalamins may be defined as long axis or short axis polarized.

In recent years a number of sophisticated spectroscopic and theoretical techniques have been utilized to examine the role of the axial ligand in priming the Co−C bond for efficient homolysis. Resonance Raman measurements reported by Spiro and co-workers[11−14] have explored the influence of protein binding on the vibrational spectrum of the corrin ring and the effect of the axial nitrogenous ligand on the vibrational frequency of the Co−C bond. A small frequency shift from 530 cm^{-1} for AdoCbl in free solution to 524 cm^{-1} for AdoCbl bound to methylmalonyl-CoA mutase was observed, but in the presence of bound substrate or product the vibration returns to 530 cm^{-1}. A similar investigation on the enzyme glutamate mutase failed to find any influence of the protein on the Co−C bond stretching frequency.[15] In solution, the nature of the axial ligand, histidine, DMB, or even base-off at low pH, has no effect on the Co−C stretching frequency.[11,13]

The insensitivity of the Co−C bond to the trans-axial ligand has also been reported in a number of recent theoretical investigations.[16−26] Density functional studies by Andruniow et al. found a small positive correlation which was primarily electronic in nature between the Co−N axial bond length and the Co−C bond dissociation energy.[22,23,26] Jensen et al. report a similar inverse trans effect, but also note a tendency toward a "base-off" configuration with changes in the Co−C bond.[18,20,24] Finally, Dölker et al. report that the trans-axial ligand has little effect on the homolysis of the Co−C bond, but may serve to inhibit heterolysis of the bond,[21,25] a result also reported by Kozlowski and Zgierski.[19] Clearly, the available experimental and theoretical data do not support the hypothesis of a strong steric or electronic influence of the trans-axial ligand on the strength of the Co−C bond.

To address the question of the influence of environment on the Co−C bond, we have performed a series of femtosecond to nanosecond transient absorption studies to investigate the effect of the solvent environment on the photolysis of adenosylcobalamin. Although the B_{12}-dependent enzymes function through the thermal cleavage of the Co−C bond, the photolysis of adenosylcobalamin is an effective tool to investigate some mechanistic aspects of the thermal homolysis reaction. In particular, the Cbl(II) state produced following photolysis is spectroscopically identical to the Cbl(II) species produced via thermolysis. Photolysis measurements provide a direct method to measure the geminate recombination of adenosyl radical with Cbl(II). Time-resolved investigations of the cobalamins also provide a probe of the electronic structure in the regions away from the vertical Franck−Condon transition observed in the ordinary absorption spectrum. A number of theoretical studies have considered the electronic structure of cobalamins with the aim of understanding the observed absorption spectrum.[27−32] However, the differences observed in the absorption spectra of various cob(III)alamin (Cbl(III)) compounds are relatively subtle, and the observed photochemistry provides an additional probe of the electronic structure as a function of ligand and solvent.

In previous work we have used ultrafast spectroscopic techniques to explore the mechanism for photolysis of both AdoCbl and the related B_{12} coenzyme methylcobalamin (MeCbl).[33−36] In complementary studies we have also investigated the photochemistry of the synthetic alkylcobalamin analogues ethylcobalamin and *n*-propylcobalamin.[37] In this paper we report the extension of these investigations to the protein environment in glutamate mutase. A preliminary report of this work appeared earlier.[38]

Glutamate mutase catalyzes the carbon-skeletal rearrangement of L-glutamate to L-*threo*-3-methylaspartate, and is one of the best-characterized AdoCbl-dependent enzymes. A high-resolution crystal structure has been solved with both the coenzyme and substrates bound in the active site.[9,39] Kinetic studies have established the chemical mechanism of the enzyme[40−43] and determined the rates at which key intermediates are formed on the enzyme. Studies on active site mutants have begun to reveal the roles of various residues in controlling the reaction. In particular, stopped flow spectroscopy has been used to measure rate constants for the substrate-initiated homolysis of AdoCbl on the enzyme.[44,45] These factors make glutamate mutase an excellent system for detailed ultrafast spectroscopic investigations to study how protein−coenzyme interactions may change the reactivity of AdoCbl.

II. Experimental Methods

A. Transient Absorption Measurements. Transient absorption measurements were performed using a self-mode-locked titanium:sapphire oscillator, running at 88 MHz and producing 20 fs, 2 nJ pulses. These pulses were amplified in a multipass amplifier. The resulting laser beam was centered at approximately 800 nm, providing 400 μJ, 50 fs pulses at a 1 kHz repetition rate. Tunable probe pulses were generated by sending the 800 nm laser pulse into a home-built noncollinear optical parametric amplifier (NOPA) constructed according to the

design of Riedle and co-workers.[46] For the present set of measurements the output consisted of 100−200 fs pulses centered at peak wavelengths between 470 and 600 nm inclusive. At each wavelength a 10 nm band-pass interference filter was used to limit the spectral bandwidth of the probe pulse. For all measurements reported in this paper the excitation wavelength is 400 nm. The polarizations of the pump and probe beams were set at the magic angle of 54.7° with respect to each other.

For kinetic measurements the probe pulses were delayed with respect to the pump pulses by a 1.5 m computer-controlled motorized translation stage (Newport-Klinger). This stage allows measurements to be made with femtosecond resolution (1 μm step size equals 6.7 fs of delay) out to a maximum time delay of ca. 10 ns. Traces were collected from −10 ps to +9 ns using 416 variable time steps. Time steps of 0.1 ps (from −10 to +5 ps), 0.2 ps (from 5 to 10 ps), 0.5 ps (from 10 to 20 ps), 1 ps (from 20 to 50 ps), 2 ps (from 50 to 100 ps), 5 ps (from 100 to 200 ps), 10 ps (from 200 to 500 ps), 20 ps (from 500 ps to 1 ns), 50 ps (from 1 to 2 ns), and 100 ps (from 2 to 9 ns) were used for the protein measurements. The reduction in the number of time steps from 811 used for cobalamins in solution[35] to 416 used for the protein sample is necessitated by the relatively short active life of the protein sample.

B. Enzyme Preparation. These experiments used the engineered "single-subunit" glutamate mutase, designated GlmES, which was expressed and purified as a recombinant protein from *E. coli* as described previously.[47] In this protein, the two subunits of the wild-type enzyme are genetically fused together so that the N terminus of the S subunit is joined to the C terminus of the E subunit by an 11 amino acid linker. GlmES has catalytic properties very similar to those of the wild-type two-subunit enzyme, but the kinetics of AdoCbl binding are simplified, thereby facilitating kinetic and spectroscopic measurements on the protein.

For transient absorption measurements, an excess of GlmES protein in 50 mM potassium phosphate buffer, pH 7.0, was reconstituted with AdoCbl immediately prior to the transient absorption scans. The final concentration of the reconstituted protein was sufficient to provide an optical density between 0.3 and 0.4 at 400 nm in a 1 mm path length quartz cell. Samples of GlmES, 3 mL, were circulated using a small-volume flow cell and a peristaltic pump. The sample reservoir was kept in an ice bath to hinder thermal denaturation of the enzyme. UV−vis absorption spectra of the protein sample obtained before and after laser exposure were essentially identical, ensuring a minimal sample degradation or production of long-lived photoproducts. In addition, activity measurements of a protein sample before and after 2 h of laser exposure demonstrated that the protein was still active with only minimal degradation after exposure to the laser.

A direct comparison between enzyme-bound AdoCbl and AdoCbl in aqueous solution was made for each probe wavelength. A sample of aqueous AdoCbl was prepared by dissolving 9.5 mg of AdoCbl in 10 mL of deoxygenated water. Half of this sample was used before the measurement on the protein sample to ensure that the sample system and delay stage were properly aligned, and half of the sample was used after the measurement on the protein sample to ensure that the alignment was still good. The signals obtained on these two samples were identical within the intrinsic noise of the transient absorption spectrometer.

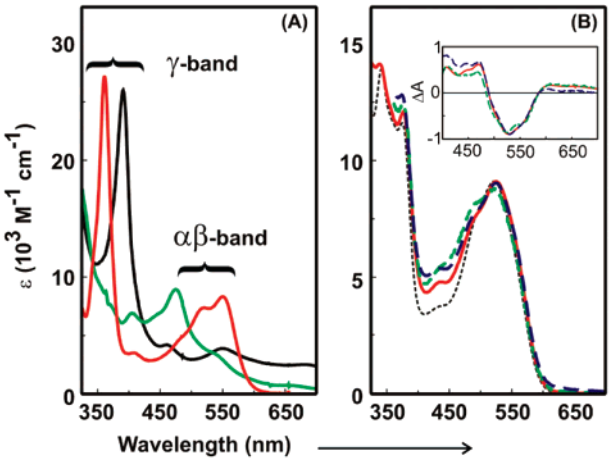

Figure 3. (A) Absorption spectrum of cob(I)alamin (black), cob(II)alamin (green), and cyanocobalamin (red) in aqueous solution. The absorption bands are labeled with the traditional nomenclature. (B) Absorption spectra of AdoCbl in aqueous solution (red line), bound to glutamate mutase (blue dashed line), and in ethylene glycol (green dashed line). The gray dotted line is the spectrum of methylcobalamin in aqueous solution. The difference spectra for the formation of Cbl(II) from AdoCbl are shown in the inset. The difference spectra in water and ethylene glycol were obtained by photolysis in the presence of a radical scavenger.[36] The GlmES difference spectrum was obtained by taking the difference between AdoCbl bound to GlmES with and without substrate.[48] At steady state in the presence of substrate ca. 25−50% of the AdoCbl forms Cbl(II).

III. Results and Discussion

A. Steady-State Absorption Spectra. The UV−vis absorption spectra of cobalamin cofactors are characteristic of the oxidation state, axial ligation, and environment. This dependence is illustrated in Figure 3, where absorption spectra of the three principal oxidation states of cobalamin are shown in part A, and the absorption spectra of AdoCbl obtained in water and ethylene glycol and bound to glutamate mutase are shown in part B. The changes observed in the absorption spectrum of AdoCbl in water and ethylene glycol and bound to glutamate mutase are subtle. To quantify the changes that are observed, a least-squares Gaussian peak fit was performed for each Cbl(III) absorption spectrum. The results of this fit for the AdoCbl absorption band as a function of solvent are shown in Figure 4.

At least four Gaussian bands are required to model the visible absorption spectrum. The lowest two bands or $\alpha\beta$ bands in alkylcobalamins and other cob(III)alamins are generally assigned as vibronic bands of the HOMO → LUMO transition.[49,50] An additional transition, accounting for much of the oscillator strength, lies on the high-energy side of the $\alpha\beta$ band. A change in the sign of the circular dichroism (CD) spectrum in this region suggests a different electronic origin for this band (Figure S2 in the Supporting Information of ref 20). The visible transition peaking around 23000 cm^{-1} also correlates with a change in sign in the CD spectrum. Thus, the visible absorption spectrum contains contributions from at least three distinct electronic transitions. The transitions contributing to the absorption spectra of AdoCbl in water and ethylene glycol and bound to glutamate mutase are modulated in intensity, but not in frequency.

The same three bands are identified in the spectrum of cyanocobalamin (vitamin B_{12}, CNCbl) and other Cbl(III) species, although the relative intensities vary. In particular, the ratio of intensities of the vibronic $\alpha\beta$ bands in CNCbl (ca. 7:3) is dramatically different from that observed for AdoCbl and MeCbl (ca. 1:1). Similar decompositions are found for other nonalkylcob(III)alamins, including aquacobalamin (H_2OCbl),

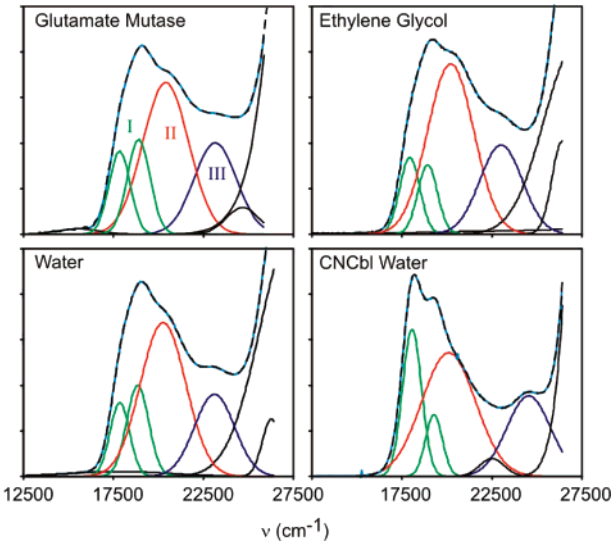

Figure 4. Least-squares Gaussian fits of the visible absorption spectra of AdoCbl bound to glutamate mutase, dissolved in ethylene glycol, and dissolved in water: (green) I, $\alpha\beta$ bands—generally assigned as vibronic transitions of one electronic transition; (red) II, 20300 cm^{-1} electronic band; (blue) III, 23000 cm^{-1} band. The spectrum of CNCbl in water is also shown for comparison.

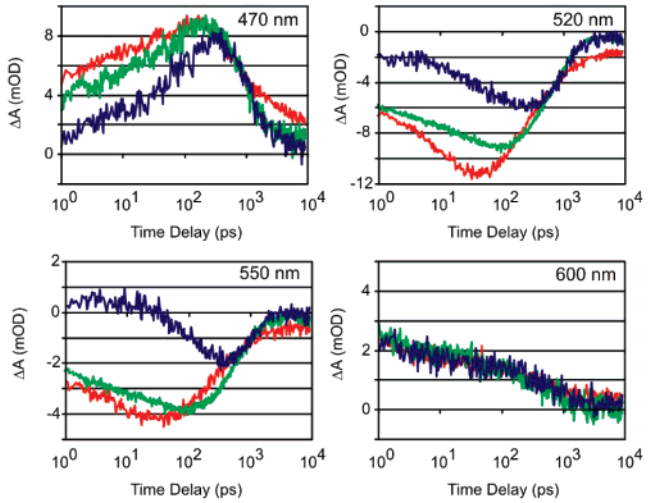

Figure 5. Transient absorption traces obtained for free AdoCbl in water (red), AdoCbl in ethylene glycol (green), and AdoCbl bound to GlmES (blue). The probe wavelengths are indicated on the panels. The traces at each probe wavelength for AdoCbl in water and AdoCbl bound to the protein were obtained under identical conditions as indicated in the text. The traces in ethylene glycol were determined in a separate experiment.[37]

hydroxocobalamin (HOCbl), and aminocobalamin (NH_3Cbl). In these Cbl(III) species the α band at ca. 540−550 nm is prominent and significantly larger than the β band.

Some additional insight into the electronic structure of cobalamins may be obtained from theoretical calculations. A number of time-dependent density functional (TD-DFT) calculations of the electronic structure and electronic spectrum of cobalamins have appeared in the literature recently.[27−32] Several of these papers report calculations for CNCbl models,[27,29,30] while two papers report calculations on a number of models including CNCbl, MeCbl, and H_2OCbl.[27,31] The consensus of the DFT calculations is similar to that reported in earlier semiempirical calculations.[49,50] The lowest energy transition, corresponding to the $\alpha\beta$ band in the observed spectrum, is the HOMO → LUMO transition, predominantly a $\pi \rightarrow \pi^*$ transition of the corrin ring, polarized along the axis running between carbons 5 and 15 in Figure 1. In this transition electron density is transferred from the axial ligands to the corrin ring.

The DFT calculations of the absorption spectra of MeCbl, H_2OCbl, and CNCbl reproduce some of the gross features of the observed absorption spectrum. In particular the calculations reproduce many of the trends observed in the γ band region in the near-UV. However, it should be noted that the calculated differences in the visible spectra of MeCbl, H_2OCbl, and CNCbl are much larger than the differences in the experimental spectra. The calculations have qualitative, but not yet quantitative, value in interpreting the observed spectra and describing the electronic structure.

B. Transient Absorption Data. Typical transient absorption traces obtained on enzyme-bound AdoCbl and free AdoCbl are compared in Figure 5. Traces were also obtained for probe wavelengths of 530, 540, 560, and 570 nm.

The overall spectral evolution for AdoCbl in water and ethylene glycol has been described in detail previously.[36] Preliminary measurements on GlmES have also been reported.[38] In all three environments the difference spectrum measured for time delays longer than a few hundred picoseconds is characteristic of the formation of Cbl(II) from AdoCbl, with a strong bleach at 520 and 550 nm and an absorption increase at 470 nm. The overall decay of the transient difference spectrum on the nanosecond time scale reflects the geminate recombination of the radical pair. For earlier time delays distinct differences are observed. In ethylene glycol the difference spectra for all time delays longer than a few picoseconds resemble the Cbl(II) difference spectrum with the small-amplitude changes assigned to vibrational and conformational relaxation. In water the bleach at 40 ps is larger than expected for the formation of Cbl(II), and resembles the difference spectrum that would be expected if the C−N bond were lengthened or broken.[36] In contrast, the data obtained for AdoCbl bound to GlmES exhibit a clear delay in the formation of the Cbl(II) radical compared with that for the coenzyme in aqueous solution or in ethylene glycol. The delayed formation of the Cbl(II) radical is particularly evident in the data obtained with a 550 nm probe where the signal indicates a small increase in absorption for the first 10 ps. An increase in absorption in this region is characteristic of formation of a Cbl(III)-type intermediate state with a prominent α band, and is not characteristic of the formation of a Cbl(II)-type state.

To analyze the spectral evolution in greater detail, the transient absorption data were fitted to a sum of exponential decay components. The data require a minimum of five exponential decay components to adequately describe the kinetics of photolysis and recombination. The initial dynamics are characterized by subpicosecond decay from the initially excited state (this region is not included in Figure 5), and a small-amplitude component characterized by an apparent rate constant of 0.16 ± 0.05 ps^{-1} ($\tau = 6$ ps). These are followed by two slower components characterized by apparent rate constants of 9.5 ± 1.0 ns^{-1} ($\tau = 105$ ps) and 1.05 ± 0.1 ns^{-1} ($\tau = 950$ ps). Finally, a small fraction of the Cbl(II) produced by photolysis does not undergo geminate recombination to AdoCbl on the longest time scale of these measurements. Although more components may be present, they are not necessary to account for the basic features of the data. The data could not be adequately fitted with fewer components. The decay-associated spectra obtained from this analysis are shown in Figure 6A.

The difference spectrum associated with each transiently formed species may be calculated from the data given a model for the dynamics.[36] A stepwise model from the initially excited

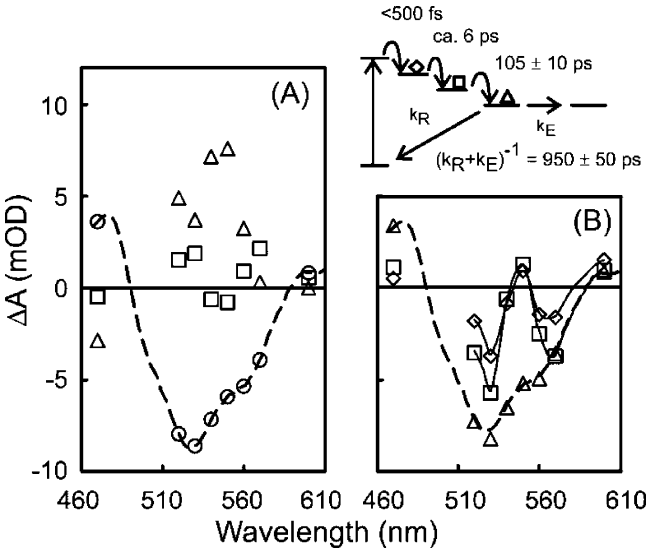

Figure 6. (A) Decay-associated difference spectra obtained from the transient absorption data: (squares) ca. 6 ps component, (triangles) 105 ± 10 ps component, (circles) 950 ps component. Dashed line: spectrum of the photoproduct at nanosecond delays as reported previously.[38] (B) Top: Stepwise model for the formation and geminate recombination of Cbl(II) radicals and following photolysis of AdoCbl bound to GlmES. Bottom: Species-associated difference spectra corresponding to the two intermediate Cbl(III) excited states (tilted squares and squares) and the geminate Cbl(II) radical (triangles). The dashed line is the expected difference spectrum for the formation of the Cbl(II) radical.

state to the final photoproduct leads to the spectra shown in Figure 6B. Bond homolysis occurs on a 105 ps time scale with the peak Cbl(II) spectrum formed approximately 320 ps after excitation. By contrast, the initial difference spectrum in ethylene glycol appears cob(II)alamin-like within 1.4 ps, and the steady-state cob(II)alamin difference spectrum develops on a time scale of ≤28 ps. In water an intermediate state with a spectrum characteristic of a base-off cobalamin is formed on a 14 ps time scale, followed by bond homolysis and formation of the radical pair spectrum on a 100 ps time scale.

The spectra corresponding to the two intermediates in Figure 6 are similar to each other, similar to the spectrum identified in our original preliminary report of studies of AdoCbl bound to GlmES, and similar to the long-lived excited-state difference spectrum observed following excitation of methylcobalamin at 520 nm.[35] These two spectra likely describe a single intermediate state, with the 6 ps decay component representing a vibrational or conformational relaxation of the molecule in the excited state. The time constant obtained in the simultaneous global analysis of all the traces appears to be a compromise between a slower time constant (ca. 10−15 ps) preferred at 520 and 530 nm near the peak of the cob(III)alamin intermediate and a faster time constant (ca. 2 ps) preferred at 470 and 560−600 nm in the wings of the spectrum. The amplitude of this component is so small at 540 and 550 nm that it is not required to fit these data. This wavelength dependence is typical of absorption changes attributed to vibrational relaxation.

The observation of a Cbl(III) intermediate state demonstrates that the protein environment changes the relative energies of the electronic states of AdoCbl and stabilizes a distinct intermediate state not observed for AdoCbl in water or ethylene glycol.[34,36] Excitation at 400 nm results in initial production of this intermediate state with unit quantum yield. The difference spectrum observed for the formation of the intermediate state from AdoCbl bound to glutamate mutase, like that observed earlier following excitation of MeCbl,[33,35] is characterized by an increase in absorption intensity between 540 and 550 nm. This spectral change corresponds to a marked increase in the intensity of the α band relative to the β band, similar to the spectra observed for σ-donating alkyl anion ligands such as CNCbl and other nonalkylcob(III)alamins. The intermediate state will have more charge density on the alkyl ligand and less charge density on the metal (i.e., a metal-to-ligand charge transfer or MLCT state).

Time-resolved spectroscopic studies of several related cobalt porphyrins have been reported previously.[51−56] In all of these studies the lack of luminescence by cobalt(II) and cobalt(III) porphyrins is attributed to rapid relaxation to a low-lying $\pi 3d_{z^2}$ or d−d state. In one study of a cobalt(III) porphyrin, Co^{III}-(octoethylporhyrin)(CN), the lowest lying excited state led to efficient CN deligation between 63 and 130 ps, via an internal conversion pathway described as $\pi\pi^* \rightarrow \pi d_{z^2} \rightarrow d_\pi d_{z^2}$.[51,52] A later femtosecond study of (tetraphenylporhyrin)Co^{II}NO demonstrated the dissociation of the NO ligand with unit quantum yield attributed to rapid internal conversion from the initially excited $\pi\pi^*$ state of the porphyrin to a low-lying, directly dissociative, $\pi 3d_{z^2}$ CT state.[53,54]

The $\pi 3d_{z^2}$ state of cobalt porpyrins and nonalkyl-Cbl(III) compounds is generally characterized as a ligand-to-metal charge transfer (LMCT) state (corrin $\pi \rightarrow$ Co) in contrast to the apparent MLCT state observed following excitation of several alkylcobalamins, including AdoCbl bound to GlmES. On the other hand, a significant difference between the molecular orbitals calculated for MeCbl and those calculated for H_2OCbl and CNCbl is a substantial mixing of the Me $2p_z$ and Co $3d_{z^2}$ orbitals.[27] Thus, the so-called Co $3d_{z^2}$ orbital at the vertical geometry is characterized in these three models as 62% Co, 6% H_2O; 57% Co, 11% CN; and 49% Co, 22% Me. This trend, increasing the electron density on the alkyl ligand, may account for the MLCT character of the intermediate excited state in alkylcobalamins.

C. Geminate Recombination. In addition to the effect on the intermediate states observed in the photoinduced homolysis reaction, the protein also influences both the intrinsic recombination rate for the geminate radical pair and the caging of the adenosyl radical. For the model in Figure 6 the quantum yield for formation of the long-lived cob(II)alamin species vs prompt geminate recombination is obtained from the rate constants and amplitudes using

$$\phi = \frac{QR}{1 + QR}$$

where the constant Q is given by

$$Q = \frac{k_1 k_2 k_3}{(k_1 - k_4)(k_2 - k_4)(k_3 - k_4)}$$

and R is the ratio of the amplitude of the long-lived cob(II)-alamin signal to the amplitude of the 950 ps decay attributed to geminate recombination. From this analysis, the quantum yield for the formation of stable radical pairs in the enzyme is $\phi = 0.05 \pm 0.03$ and the resulting intrinsic rate constant for geminate recombination is 1.0 ± 0.1 ns^{-1}. In contrast, the intrinsic rate constant for recombination in water, ethylene glycol, and mixtures of water and ethylene glycol is 1.4 ns^{-1} ($\tau = 714$ ps).[36] Thus, the protein has reduced the rate constant for recombination by ∼30%. This reduction in rate constant may reflect a modest stabilization of the radical pair by the protein, but is insufficient to account for the $\sim 10^{12}$-fold increase in the homolysis rate observed when substrate is bound to the protein. The quantum

yield for formation of the long-lived radical pair and the rate constant for "cage escape" by the adenosyl radical, 0.05 ± 0.03 ns^{-1}, are similar to those observed for AdoCbl in ethylene glycol. Thus, while the protein provides a cage to prevent diffusive loss of the adenosyl radical, it appears that the ultimate yield for long-lived radicals is determined by the evolution from a singlet to a triplet radical pair as proposed for AdoCbl in ethylene glycol.

IV. Conclusions

We have shown that the photochemistry of adenosylcobalamin is dependent upon the environment of the cofactor. When dissolved in water, the initial photochemistry results in the formation of an intermediate state with a spectrum characteristic of the dissociation of the axial DMB ligand. Formation of Cbl(II) follows on a 100 ps time scale. Excitation of AdoCbl bound to glutamate mutase results in formation of an MLCT intermediate state which decays to form Cbl(II) on a 105 ps time scale. Finally, excitation in ethylene glycol results in prompt bond homolysis with no indication of either a base-off or an MLCT intermediate state. The differences observed in the photodissociation pathway do not correlate with changes in the linear absorption spectrum, but rather reflect changes in the relative energies of the electronic states in regions away from the Franck−Condon region. The electronic states appear to change significantly as a function of alkyl group and axial base coordination. These findings raise the intriguing possibility that the protein may influence the excited states of the cofactor rather than the ground state, which could be important for the activation of the Co−C bond toward homolysis by the enzyme.

From an analysis of the geminate recombination process, the quantum yield for the formation of stable radical pairs in the enzyme is found to be $\phi = 0.05 \pm 0.03$ and the resulting intrinsic rate constants for geminate recombination and cage escape are 1.0 ± 0.1 and 0.05 ± 0.03 ns^{-1}, respectively. The protein has reduced the rate constant for prompt recombination by ~30%, which may reflect a modest stabilization of the radical pair by the protein, but is not sufficient to account for the increase in the homolysis rate observed when substrate is bound to the protein. The quantum yield for formation of the long-lived radical pair and the rate constant for cage escape by the adenosyl radical are similar to those observed for adenosylcobalamin in ethylene glycol. Thus, while the protein provides a cage to prevent diffusive loss of the adenosyl radical, it appears that the ultimate yield for long-lived radicals is determined by the evolution from a singlet to a triplet radical pair as proposed for AdoCbl in ethylene glycol.

Acknowledgment. This work was supported by grants from the NSF (CHE 0078972) and from the NIH (GM59227 and DK53842).

References and Notes

(1) Banerjee, R. *Chem. Rev.* **2003**, *103*, 2083−2094.
(2) Toraya, T. *Chem. Rev.* **2003**, *103*, 2095−2127.
(3) Marsh, E. N. G.; Drennan, C. L. *Curr. Opin. Chem. Biol.* **2001**, *5*, 499−505.
(4) Finke, R. G.; Hay, B. P. *Inorg. Chem.* **1984**, *23*, 3041−3043.
(5) Garr, C. D.; Finke, R. G. *Inorg. Chem.* **1993**, *32*, 4414−4421.
(6) Hay, B. P.; Finke, R. G. *Polyhedron* **1988**, *7*, 1469−1481.
(7) Marsh, E. N. G.; Ballou, D. P. *Biochemistry* **1998**, *37*, 11864−11872.
(8) Masuda, J.; Shibata, N.; Morimoto, Y.; Toraya, T.; Yasuoka, N. *Structure* **2000**, *8*, 775−788.
(9) Reitzer, R.; Gruber, K.; Jogl, G.; Wagner, U. G.; Bothe, H.; Buckel, W.; Kratky, C. *Structure* **1999**, *7*, 891−902.
(10) Mancia, F.; Keep, N. H.; Nakagawa, A.; Leadlay, P. F.; McSweeney, S.; Rasmussen, B.; Bösecke, P.; Diat, O.; Evans, P. R. *Structure* **1996**, *4*, 339−350.
(11) Dong, S.; Padmakumar, R.; Banerjee, R.; Spiro, T. G. *J. Am. Chem. Soc.* **1996**, *118*, 9182−9183.
(12) Dong, S.; Padmakumar, R.; Banerjee, R.; Spiro, T. G. *J. Am. Chem. Soc.* **1999**, *121*, 7063−7070.
(13) Dong, S.; Padmakumar, R.; Banerjee, R.; Spiro, T. G. *Inorg. Chim. Acta* **1998**, *270*, 392−398.
(14) Dong, S.; Padmakumar, R.; Maiti, N.; Banerjee, R.; Spiro, T. G. *J. Am. Chem. Soc.* **1998**, *120*, 9947−9948.
(15) Huhta, M. S.; Chen, H.-P.; Hemann, C.; Hille, C. R.; Marsh, E. N. G. *Biochem. J.* **2001**, *355*, 131−137.
(16) Rutkowska-Zbik, D.; Jaworska, M.; Witko, M. *Struct. Chem.* **2004**, *15*, 431−435.
(17) Randaccio, L.; Geremia, S.; Stener, M.; Toffoli, D.; Zangrando, E. *Eur. J. Inorg. Chem.* **2002**, 93−103.
(18) Jensen, K. P.; Sauer, S. P. A.; Liljefors, T.; Norrby, P.-O. *Organometallics* **2001**, *20*, 550−556.
(19) Kozlowski, P. M.; Zgierski, M. Z. *J. Phys. Chem. B* **2004**, *108*, 14163−14170.
(20) Jensen, K. P.; Ryde, U. *J. Phys. Chem. A* **2003**, *107*, 7539−7545.
(21) Dolker, N.; Maseras, F.; Lledos, A. *J. Phys. Chem. B* **2003**, *107*, 306−315.
(22) Andruniow, T.; Zgierski, M. Z.; Kozlowski, P. M. *J. Am. Chem. Soc.* **2001**, *123*, 2679−2680.
(23) Andruniow, T.; Zgierski, M. Z.; Kozlowski, P. M. *Chem. Phys. Lett.* **2000**, *331*, 509−512.
(24) Jensen, K. P.; Ryde, U. *J. Mol. Struct.: THEOCHEM* **2002**, *585*, 239−255.
(25) Dolker, N.; Maseras, F.; Lledos, A. *J. Phys. Chem. B* **2001**, *105*, 7564−7571.
(26) Andruniow, T.; Zgierski, M. Z.; Kozlowski, P. M. *J. Phys. Chem. B* **2000**, *104*, 10921−10927.
(27) Stich, T. A.; Brooks, A. J.; Buan, N. R.; Brunold, T. C. *J. Am. Chem. Soc.* **2003**, *125*, 5897−5914.
(28) Jaworska, M.; Lodowski, P. *J. Mol. Struct.: THEOCHEM* **2003**, *631*, 209−223.
(29) Ouyang, L.; Randaccio, L.; Rulis, P.; Kurmaev, E. Z.; Moewes, A.; Ching, W. Y. *J. Mol. Struct.: THEOCHEM* **2003**, *622*, 221−227.
(30) Andruniow, T.; Kozlowski, P. M.; Zgierski, M. Z. *J. Chem. Phys.* **2001**, *115*, 7522−7533.
(31) Brooks, A. J.; Vlasie, M.; Banerjee, R.; Brunold, T. C. *J. Am. Chem. Soc.* **2004**, *126*, 8167−8180.
(32) Stich, T. A.; Buan, N. R.; Brunold, T. C. *J. Am. Chem. Soc.* **2004**, *126*, 9735−9749.
(33) Walker, L. A., II; Jarrett, J. T.; Anderson, N. A.; Pullen, S. H.; Matthews, R. G.; Sension, R. J. *J. Am. Chem. Soc.* **1998**, *120*, 3597−3603.
(34) Walker, L. A., II; Shiang, J. J.; Anderson, N. A.; Pullen, S. H.; Sension, R. J. *J. Am. Chem. Soc.* **1998**, *120*, 7286−7292.
(35) Shiang, J. J.; Walker, L. A., II; Anderson, N. A.; Cole, A. G.; Sension, R. J. *J. Phys. Chem. B* **1999**, *103*, 10532−10539.
(36) Yoder, L. M.; Cole, A. G.; Walker, L. A., II; Sension, R. J. *J. Phys. Chem. B* **2001**, *105*, 12180−12188.
(37) Cole, A. G.; Yoder, L. M.; Shiang, J. J.; Anderson, N. A.; Walker, L. A., II; Banaszak Holl, M. M.; Sension, R. J. *J. Am. Chem. Soc.* **2002**, *124*, 434−441.
(38) Sension, R. J.; Cole, A. G.; Harris, A. D.; Fox, C. C.; Woodbury, N. W.; Lin, S.; Marsh, E. N. G. *J. Am. Chem. Soc.* **2004**, *126*, 1598−1599.
(39) Gruber, K.; Reitzer, R.; Kratky, C. *Angew. Chem., Int. Ed.* **2001**, *40*, 3377−3380.
(40) Chih, H.-W.; Marsh, E. N. G. *J. Am. Chem. Soc.* **2000**, *122*, 10732−10733.
(41) Chih, H.-W.; Marsh, E. N. G. *Biochemistry* **2001**, *40*, 13060−13067.
(42) Cheng, M.-C.; Marsh, E. N. G. *Biochemistry* **2004**, *43*, 2155−2158.
(43) Cheng, M.-C.; Marsh, E. N. G. *Biochemistry* **2005**, *44*, 2686−2691.
(44) Madhavapeddi, P.; Ballou, D. P.; Marsh, E. N. G. *Biochemistry* **2002**, *41*, 15803−15809.
(45) Huhta, M. S.; Ciceri, D.; Golding, B. T.; Marsh, E. N. G. *Biochemistry* **2002**, *41*, 3200−3206.
(46) Wilhelm, T.; Piel, J.; Riedle, E. *Opt. Lett.* **1997**, *22*, 1494−1496.
(47) Chen, H.-P.; Marsh, E. N. G. *Biochemistry* **1997**, *36*, 14939−14945.
(48) Chen, H.-P.; Marsh, E. N. G. *Biochemistry* **1997**, *36*, 7884−7889.
(49) Day, P. *Coord. Chem. Rev.* **1967**, *2*, 99−108.
(50) Fugate, R. D.; Chin, C.-A.; Song, P.-S. *Biochim. Biophys. Acta* **1976**, *421*, 1−11.
(51) Tait, C. D.; Holten, D.; Gouterman, M. *Chem. Phys. Lett.* **1983**, *100*, 268−272.
(52) Tait, C. D.; Holten, D.; Gouterman, M. *J. Am. Chem. Soc.* **1984**, *106*, 6653−6659.

(53) Morlino, E. A.; Rodgers, M. A. J. *J. Am. Chem. Soc.* **1996**, *118*, 11798−11804.
(54) Morlino, E. A.; Walker, L. A., II; Sension, R. J.; Rodgers, M. A. J. *J. Am. Chem. Soc.* **1995**, *117*, 4429−4430.
(55) Yu, H. Z.; Baskin, J. S.; Steiger, B.; Wan, C. Z.; Anson, F. C.; Zewail, A. H. *Chem. Phys. Lett.* **1998**, *293*, 1−8.
(56) Loppnow, G. R.; Melamed, D.; Leheny, A. R.; Hamilton, A. D.; Spiro, T. G. *J. Phys. Chem.* **1993**, *97*, 8969−8975.